Novel 60 GHz Band Spatial Synthetic Exposure System for Investigating Thermal Physiological Responses to Simultaneous Localized Millimeter-Wave Exposure at Multiple Skin Points

Sakura Tsuruga, Takashi Hikage, Hiroshi Masuda, Tatsuya Ishitake, Kun Li, and Akiko Nagai

Abstract – A novel 60 GHz band exposure system was developed for studying thermal physiological responses and cellular functions to millimeter-wave (MMW) localized exposure at multiple points. To achieve a highly localized exposure system operating at 60 GHz in the desired area, the authors proposed a spatial synthetic beamtype setup consisting of dielectric lens antennas capable of irradiating focused beams. This system uses radio wave interference and phase differences to achieve simultaneous localized exposure at multiple sites. Experiments were conducted by using an arm phantom to measure temperature increases, confirming the system's ability to simultaneously induce high-intensity exposure at multiple locations. The developed system enabled efficient and precise exposure control in experiments aimed at exploring the biological effects of local MMW exposure at multiple sites in human volunteer studies. This approach could be used for human experiments but at this time is studied with phantoms.

1. Introduction

The use of radio waves in the quasi-millimeter-wave (qMMW) and millimeter-wave (MMW) spectrum is rapidly advancing. Despite this progress, there remains a significant gap in biological evidence concerning exposure to qMMW and MMW radiation [1]. Obtaining research on biologically plausible effects and reliable experimental data is crucial for revising international safety guidelines regarding radio wave exposure in frequency bands beyond the MMW range.

Manuscript received 21 September 2024. This work was conducted under the project "Study on the Biological Effects on Thermal Physiology and Cellular Functions during Millimeter-Wave Exposure" by Ministry of Internal Affairs and Communications of Japan. Grant Number JPMI10001.

Hiroshi Masuda and Tatsuya Ishitake are with the Kurume University School of Medicine, 67 Asahi-Machi, Kurume, Fukuoka, 8300011 Japan.

Sakura Tsuruga and Takashi Hikage are with the Faculty of Information Science and Technology, Hokkaido University, Kita 14, Nishi 9, Kita-ku, Sapporo, Hokkaido, 0600814 Japan; e-mail: {tsuruga, hikage}@wtemc.ist.hokudai.ac.jp.

Kun Li is with the University of Electro-Communications, 1-5-1 Chofugaoka, Chofu-shi, Tokyo, 1828585 Japan.

Akiko Nagai is with Aichi Gakuin University, 12 Araike, Iwasaki-cho, Nisshin, Aichi 4700195 Japan.

The index used as the standard value for biological effects in the middle-frequency and high-frequency bands that have traditionally been used for mobile communications is the specific absorption rate. The International Commission on Non-Ionizing Radiation Protection (ICNIRP) and the Institute of Electrical and Electronics Engineers (IEEE) have each published guidelines [2–4]. This index is based on assessment of basic effects of exposure of the human body to electromagnetic fields, such as rise in core body temperature, localized temperature rise, and associated pain, and this is a conservative standard. For the previously mentioned qMMW and MMW, power density (ICNIRP2020: transmitted power density; IEEE2019: incident power density and skin power density) is used as the standard value.

In the past, safety studies, such as simulations of temperature rise in the human head [5] and of the power absorption of a phantom near a LAN router [6] were conducted. Considering the future expansion of use, it is extremely important to conduct research on the biological effects of exposure to radio waves in the MMW band and higher on the human body and to obtain reliable experimental data.

To address this need, we focused our efforts on the 60 GHz band and developed an exposure system specifically designed for animal and human volunteer experiments. In this article, we report the results of our development. A key feature of the system is its ability to achieve simultaneous localized exposure at multiple points on the skin by using radio wave interference and phase differences. To verify the performance of the developed system, temperature rise measurements were conducted using a skin-simulating phantom.

2. Development of the Exposure System

Human volunteer experiments aimed at collecting and analyzing thermal physiological indices, such as the rise in body temperature and changes in skin blood flow, resulting from exposure to 60 GHz MMW. The experiments were conducted in an artificial climate chamber where temperature and humidity were controlled, and the surface temperature of the human body and physiological indicators in response to radio wave exposure were measured. In addition, this study also conducted animal experiments using a live rat to clarify the dose–

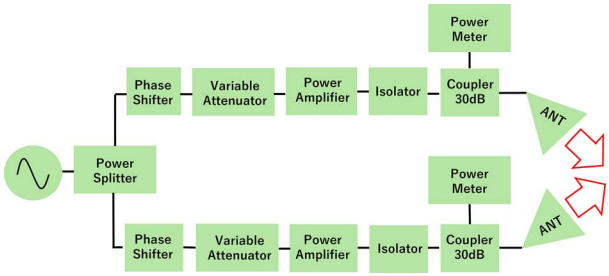

Figure 1. Block diagram of exposure setup.

response relationship of skin inflammatory reactions due to MMW exposure. In preparation for human volunteer experiments and animal experiments, a phantom evaluation was performed.

We have previously verified the ability to achieve intense exposure in specific target areas by using a system that spatially synthesizes radio waves through two dielectric lens antennas [7]. The block diagram is shown in Figure 1, and the overview of the spatial synthetic exposure system is shown in Figure 2. This spatial synthetic exposure system can achieve high-intensity localized exposure in a desired area by synthesizing radio waves from two lens antennas in space. A notable feature of this device is that the two lens antennas cause

Figure 2. Overview of spatial synthetic exposure system.

Table 1. Analysis conditions[a]

Analysis region (mm)	1849 × 1629 × 835
Number of cells (Gcells)	2.515
Cell size (mm)	0.05–0.25
Frequency (GHz)	60
Simulation periods	300
Boundary condition	10 layers UPML

[a] Gcells, giga cells; UPML, uniaxial perfectly matched layers.

interference between each other, depending on the polarization of the antennas, making it possible to simultaneously expose multiple locations in addition to uniform exposure to a single location.

We performed simulations to evaluate the exposure pattern due to interference between two lens antennas. The analysis in this study was performed by using commercially available finite-difference time-domain (FDTD) analysis software (Sim4Life, version 6.2.0.4280, Schmid & Partners Engineering AG, Zürich, Switzerland). A plane phantom with size 200 mm × 200 mm × 10 mm was used as the target. The FDTD simulation settings are shown in Table 1, and the electrical constants are shown in Table 2. The power density distribution obtained by the analysis is shown in Figures 3 and 4. When the polarizations were orthogonal, uniform exposure occurred in a single location, as shown in Figure 3a, whereas when the polarizations were identical, interference fringes appeared in the exposed area, as shown in Figure 3b. Interference fringes cause the electric fields to reinforce each other at regular intervals, resulting in high-intensity exposure at multiple locations. In addition, as shown in Figure 4, we confirmed through simulation that it is possible to change the exposure pattern because the interference fringes vary, depending on the phase difference between each lens antenna. Therefore, we planned to use these interference fringes to conduct simultaneous localized exposure experiments at multiple locations.

3. Performance Measurement

To confirm whether exposure to a single location and multiple locations is feasible using the developed exposure device, surface temperature rise measurements were carried out using an arm-shaped phantom. In this experiment, an arm-shaped phantom was placed at 300 mm, which is the focal length of the exposure device, and localized exposure to a single location with orthogonally polarized waves, and simultaneous exposure to multiple locations with the same polarized wave were evaluated by measuring the surface temperature rise using a

Table 2. Electrical constants[a]

	Relative permittivity	Electrical conductivity
Dielectric lens (PTFE)	2.1	1
Housing	PEC	
Phantom (skin at 60 GHz)	7.975	36.4

[a] PTFE, polytetrafluoroethylene; PEC, perfect electric conductor.

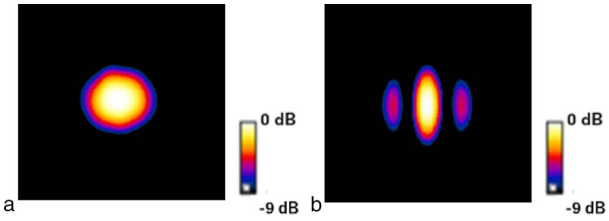

Figure 3. Power density distribution for each polarization. (a) orthogonal, (b) identical.

thermal camera (FLIR T530, Teledyne FLIR LLC, Wilsonville, Oregon, USA). The arm-shaped phantom used in the experiment was designed to match the electrical constants of human skin (dry) at 60 GHz (Figure 5). The electrical constants values are shown in Table 3. The shape and dimensions are based on the arm of an average Japanese numerical human body model. The surface after molding is flat, and the effects of reflections during exposure due to surface roughness are negligible.

The experimental conditions for this measurement are shown in Table 4. The exposure time was set to 900 s to allow sufficient temperature rise. The antenna input power was carried out under the three conditions shown in Table 4. When exposed to orthogonally polarized waves, orthogonal polarization was achieved by changing the left-hand waveguide to a cross tube and the right-hand waveguide to a straight tube when looking at the exposure device from the front. The phase difference can be changed by a phase shifter installed in the exposure device. In this measurement, it was set to 0 rad and π rad. The temperature increase was evaluated at the pixel with the maximum temperature increase after 900 s.

Figure 6 shows the images obtained by the thermal camera when emitting orthogonally polarized and the same polarized waves. When exposed to orthogonally polarized waves, a single localized exposure was observed, whereas when exposed to the same polarized wave,

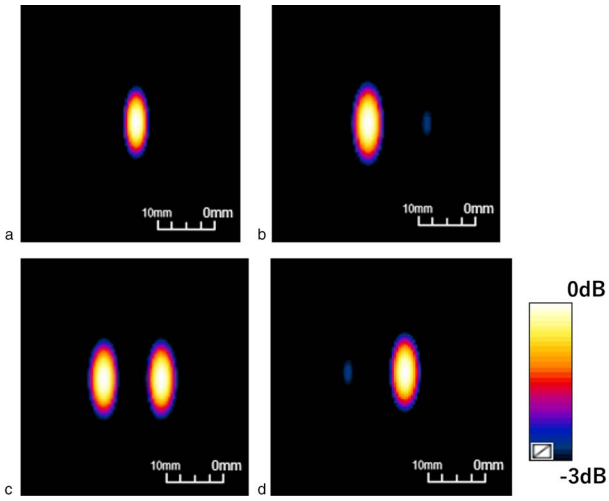

Figure 4. Power density distribution for each phase difference at the same polarization. (a) 0 rad, (b) $\pi/2$ rad, (c) π rad, (d) $3\pi/2$ rad.

Figure 5. Arm-shaped phantom.

exposure to multiple locations was observed due to interference fringes such as the analysis results previously shown. The temperature rise graph shown in Figure 7, confirms that there is a correlation between the antenna input power and the temperature rise in both the orthogonal and same polarized cases. In addition, when comparing the same polarized and orthogonally polarized waves, the temperature rise value in the same polarized wave was about 1.5 times higher. This is thought to be because electric field reinforcement occurs in the same polarization, and the maximum absorbed power density on the arm-shaped phantom surface is larger than that in the orthogonal polarization. On the other hand, the temperature rise characteristics for each phase difference when the polarization is the same showed a larger temperature rise value when the phase difference was π rad. These results show that the developed exposure device can achieve localized exposure at a single location and multiple locations. In addition, it was confirmed that the same polarized exposure allows for higher intensity exposure than the orthogonally polarized exposure.

4. Conclusion

In this article, we devised a novel spatially compound exposure system, the first of its kind, enabling the observation of thermal thresholds for physiological indicators, such as skin surface temperature, skin blood flow, and sweat rate, during localized MMW exposure in human volunteer experiments and successfully achieved the desired performance. This system is notable for its ability to achieve simultaneous localized exposure at

Table 3. Condition of skin

	Relative permittivity	Loss tangent
Skin, dry	7.9	1.4

Table 4. Experimental conditions

Frequency (GHz)	60
Exposure time (s)	900
Antennas input power (W)	0.5 W for each antenna 1 W for each antenna 2 W for each antenna
Polarization	Orthogonal, same
Phase difference in the same polarization (rad)	0, π

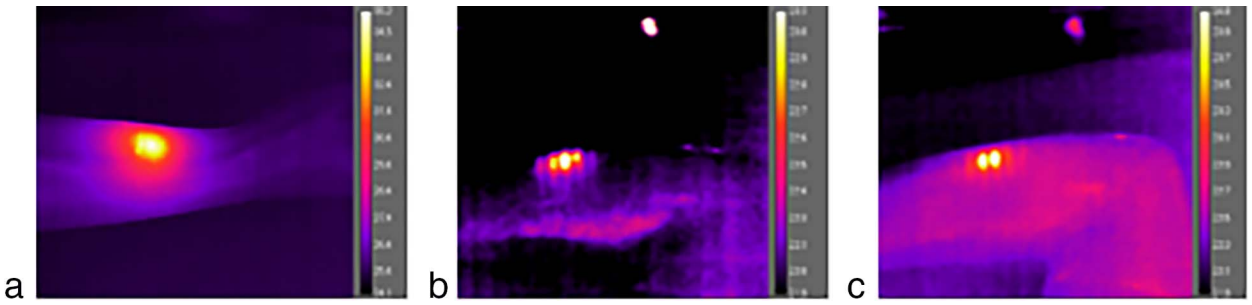

Figure 6. Thermal images of the arm-shaped phantom: (a) orthogonal polarization, (b) phase difference of 0 rad for identical polarization, and (c) phase difference of π rad for identical polarization.

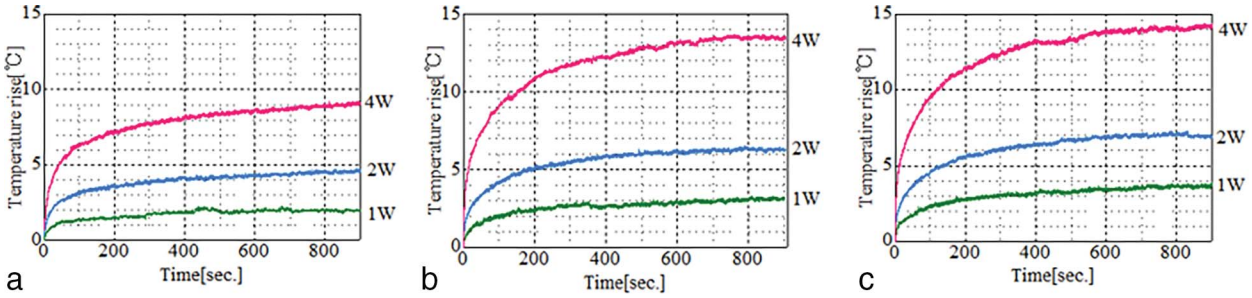

Figure 7. Peak temperature rise characteristics for: (a) orthogonal polarization, (b) phase difference of 0 rad for identical polarization, and (c) phase difference of π rad for identical polarization.

multiple points on the skin. Temperature rise experiments by using an arm-shaped phantom confirmed the system's ability to focus exposure at a single location with orthogonally polarized waves, as well as to induce temperature increases from simultaneous exposure at multiple locations using the same polarized wave. In experiments with the same polarized wave, it was confirmed that the interference fringes could be controlled by adjusting the phase difference between each lens antenna by using a phase shifter. Furthermore, when comparing the same polarized wave with orthogonally polarized waves, it was found that the temperature rise with the same polarized wave was approximately 1.5 times higher.

In the future, we plan to use this innovative spatial synthetic exposure system, with its capability for simultaneous multipoint skin exposure, to measure physiological indices and temperature rise data, contributing to the revision of current protection guidelines regarding the effects of radio wave exposure on the human body.

5. References

1. World Health Organization, "WHO Research Agenda for Radiofrequency Fields," https://iris.who.int/bitstream/handle/10665/44396/9789241599948_eng.pdf (Accessed 11 November 2024).
2. International Commission on Non-Ionizing Radiation Protection, "Guidelines for Limiting Exposure to Electromagnetic Fields (100 kHz to 300 GHz)," *Health Physics*, **118**, 5, May 2020, pp. 483-524.
3. International Commission on Non-Ionizing Radiation Protection, "International Commission on Non-Ionizing Radiation Protection Guidelines for Limiting Exposure to Time-Varying Electric and Magnetic Fields (1 Hz to 100 kHz)," *Health Phys*, **99**, 6, December 2010, pp. 818-836.
4. IEEE International Committee on Electromagnetic Safety, "IEEE Standard for Safety Levels With Respect to Human Exposure to Radio Frequency Electromagnetic Fields, 0 Hz to 300 GHz," IEEE Std C95.1-2019, October 2019, pp. 1-312.
5. S. Kodera, J. G. Tames, and A. Hirata, "Temperature Elevation in the Human Brain and Skin With Thermoregulation During Exposure to RF Energy," *BioMedical Engineering Online*, **17**, 1, January 2018, pp. 1-17.
6. K. Saito, K. Nishino, R. Takei, T. Nagaoka, S. Watanabe, et al., "SAR Evaluations of Phantom Surface Close to Antenna for Wireless LAN Router," 2018 International Workshop on Antenna Technology, Nanjing, China, March 5–7, 2018, pp. 1-2.
7. T. Hikage, R. Ozaki, T. Ishitake, and H. Masuda, "Novel 60 GHz Band Spatial Synthetic Exposure Setup to Investigate Biological Effects of 5G and Beyond Wireless Systems on Human Body," *Frontiers in Public Health*, **9**, December 2021, pp. 1-11.